

TRAPPC11-related muscular dystrophy with hypoglycosylation of alpha-dystroglycan in skeletal muscle and brain.

Pinki Munot

Great Ormond Street Hospital For Children NHS Foundation Trust

Nadine McCrea

Great Ormond Street Hospital For Children NHS Foundation Trust

Silvia Torelli

University College London Great Ormond Street Institute of Child Health

Adnan Manzur

Great Ormond Street Hospital For Children NHS Foundation Trust

Caroline Sewry

University College London Queen Square Institute of Neurology

Darren Chambers

University College London Queen Square Institute of Neurology

Lucy Feng

University College London Queen Square Institute of Neurology

Pierpaolo Ala

University College London Great Ormond Street Institute of Child Health

Irina Zaharieva

University College London Great Ormond Street Institute of Child Health

Nicola Ragge

Birmingham Women's and Children's NHS Foundation Trust

Helen Roper

University Hospitals Birmingham NHS Foundation Trust

Tamas Marton

Birmingham Women's and Children's NHS Foundation Trust

Phil Cox

Birmingham Women's and Children's NHS Foundation Trust

Miroslav Milev

Concordia University Department of Biology

Michael Sacher

Concordia University Department of Biology

Wen-Chen Liang

Kaohsiung Medical University Hospital

Shinsuke Maruyama

Kagoshima University Graduate School of Medical and Dental Sciences

Ichizo Nishino

National Center for Neurology and Psychiatry

Rahul Phadke (✉ r.phadke@ucl.ac.uk)

University College London Institute of Neurology <https://orcid.org/0000-0001-9699-2718>

Francesco Muntoni

University College London Great Ormond Street Institute of Child Health

Research

Keywords: TRAPPC11, muscular dystrophy, dystroglycan, IIH6, glycosylation, cerebellum, Purkinje cell,

Posted Date: October 12th, 2020

DOI: <https://doi.org/10.21203/rs.3.rs-31937/v2>

License:   This work is licensed under a Creative Commons Attribution 4.0 International License. [Read Full License](#)

Version of Record: A version of this preprint was published at Neuropathology and Applied Neurobiology on October 14th, 2021. See the published version at <https://doi.org/10.1111/nan.12771>.

Abstract

Background: TRAPPC11, a subunit of the transport protein particle (TRAPP) complex is important for complex integrity and anterograde membrane transport from the endoplasmic reticulum (ER) to the ER-Golgi intermediate compartment. Several individuals with *TRAPPC11* mutations have been reported with muscle weakness and other features including brain, liver, skeletal and eye involvement. A detailed analysis of brain and muscle biopsies will further our understanding of the presentation and etiology of *TRAPPC11*-disease.

Methods: We describe five cases of early-onset *TRAPPC11*-related muscular dystrophy with a systematic review of muscle pathology in all five individuals, post-mortem brain pathology findings in one individual, and membrane trafficking assays in another.

Results: All affected individuals presented in infancy with muscle weakness, motor delay and elevated serum creatine kinase (CK). Additional features included cataracts, liver disease, intellectual disability, cardiomyopathy, movement disorder, and structural brain abnormalities. Muscle pathology in all five revealed dystrophic changes, universal hypoglycosylation of alpha-dystroglycan and variably reduced dystrophin-associated complex proteins. Membrane trafficking assays showed defective Golgi trafficking in one individual. Neuropathological examination of one individual revealed cerebellar atrophy, granule cell hypoplasia, Purkinje cell (PC) loss and dendritic neurodegeneration, reduced alpha-dystroglycan (IIH6) expression in PC and dentate neurons, and absence of neuronal migration defects.

Conclusions: This report suggests that recessive mutations in *TRAPPC11* are linked to muscular dystrophies with hypoglycosylation of alpha-dystroglycan. The structural brain involvement that we document for the first time resembles the pathology previously reported in N-linked congenital disorders of glycosylation (CDG) such as *PMM2*-CDG, suggesting defects in multiple glycosylation pathways in this condition.

Background

Muscular dystrophies are a heterogeneous group of disorders characterised by progressive muscle weakness with a dystrophic muscle biopsy (1). Their severity ranges from congenital muscular dystrophy (CMD) with onset within the first year of life to later onset variants, within the spectrum of limb girdle muscular dystrophies (LGMDs) (2). Multi-system involvement is a feature of several CMDs and LGMDs, particularly with structural brain abnormalities and mental retardation occurring especially in some CMDs, and cardiac involvement coexisting in several CMD and LGMD subtypes. Extracellular matrix proteins and proteins involved in glycosylation of alpha-dystroglycan are frequently involved in CMDs, while proteins located in the sarcolemma, members of the dystrophin associated protein complex (DAPC), and nuclear envelope proteins are the most common proteins involved in LGMDs. Despite significant advances, some individuals remain undiagnosed. Although there has recently been an increase in discovery of novel disease-associated genes by application of whole exome and genome sequencing (WES and WGS), understanding the molecular mechanisms underpinning these novel genes and proteins can be challenging.

In 2013, Bogershausen et al (3) described 3 families with an unusual phenotype including muscle weakness and elevated creatine kinase (CK) resembling a LGMD, but with associated dyskinesia, ataxia, and intellectual disability. Recessive mutations in the *TRAPPC11* gene were identified, leading to the description of LGMD2S. Since then, a few isolated cases affected by either LGMD2S or a more severe congenital form have been reported (4, 5). In this study, we describe five cases of muscular dystrophy associated with mutations in *TRAPPC11* and discuss a possible role of aberrant glycosylation of alpha-dystroglycan in the disease process. We also present post mortem pathology findings in one individual and membrane trafficking assays in another. The structural brain defects identified are different from those typically associated in dystroglycanopathies and more closely resemble the findings in defects of N-glycosylation disorders. Our findings broaden the phenotype and greatly improve our understanding of the pathology of *TRAPPC11*-associated disorders.

Methods

All human tissues in this study were acquired and processed under appropriate consent and institutional research ethics cover (REC reference: 13/LO/1894 (NRES Committee London). Whole exome sequence was performed on Patient 5 as part of the Deciphering Developmental Disorders (DDD) Study (Cambridge South REC ref: 10/H0305/83 and Republic of Ireland REC ref: GEN/284/12). Muscle biopsies were processed in accordance with standard protocols as previously described (6). Quantitative western blotting on muscle lysates using an antibody against alpha-dystroglycan (IIH6) and laminin overlay assay (LOL) were performed as previously described (7).

Paraffin embedded samples from the brain were sectioned at 4µm and immunohistochemistry performed on either the Ventana Benchmark Ultra or Discovery Ultra IHC Systems using the standard deparaffinisation protocol and the following antibodies and dilutions; Neurofilament Cocktail (Dako M0762) 1:500, SMI31 (BioLegend 80160) 1:5000, SMI32 (BioLegend 801701) 1:500, SMI94 (BioLegend 836504) 1:100, GFAP (DAKO Z0334) 1:2500, CD68 (Dako M0876) 1:100 and TRAPPC11 (Biorbyt ORB186301) 1:200.

Quantitative flow cytometric assay for alpha-dystroglycan was performed on cultured dermal fibroblasts from individual 1, in accordance with a procedure previously described (8). Regeneration was assessed semiquantitatively in sections by identification of fibres expressing fetal/developmental myosin heavy chains (known markers of regeneration). Necrotic fibres were identified by their loss of eosinophilia in H&E stained sections with or without myophagocytosis, and loss of staining for spectrin (indicating membrane damage).

The trafficking of VSVG-GFP ts045 and quantification of the data was performed in cultured dermal fibroblasts from individual 1 as described by Koehler et al (9). The retention using selective hooks (RUSH) assay was performed and quantified as described by Milev et al (10).

Results

Molecular genetics

Whole exome sequencing on the index case (individual 1) revealed compound heterozygous mutations in *TRAPPC11*: c.100C>T p. (Arg34*) and c.2938G>A p. (Gly980Arg). We further identified four unrelated families with four affected members who all had compound heterozygous mutations as indicated in Table 1.

Table 1: Summary of TRAPPC11 cases

Individual	1	2	3	4	5
TRAPPC11 variants	c.100C>T & c.2938G>A p.(Arg34*) & p.(Gly980Arg)	c.661-1G>T & c.2938G>A p.Leu240Alafs*10 or p.Leu240Valfs*7 & p.Gly980Arg	c.1816C>T & c.2938G>A p.Gln606X & p.Gly980Arg	c.2644delA & c.2938G>A p.G980R & p.T881fs	c.829A>G & c.2234C>A p.Lys277Glu & p.Thr745Lys
Consanguinity	N	N	N	N	N
Sex	M	F	M	F	M
Age at onset	Infancy	1 year	1 year, 6 months	Infancy	< 6 months
Age at last follow up	5.5 years	10 years	3 years, 7 months	5.0 years	Died age 32 months
Muscle involvement	Walked at 22months Proximal weakness Pseudohypertrophy Mild contractures at elbows & ankles CK 12000 IU/L	Walk at 18m/o Proximal weakness No calf hypertrophy No joint contractures CK 8699 IU/L	Walk at 18m/o Proximal weakness Mild calf hypertrophy No joint contractures CK 10043 IU/L	Walked at 18months Proximal weakness Slight pseudohypertrophy No contractures CK 2,787 IU/L	Able to roll, never achieved unsupported sitting Pseudohypertrophy of thigh and calf muscles No contractures CK 3851 IU/L
Eye	Bilateral cataracts	Bilateral cataracts	N	ND	No cataracts, strabismus
Intellectual disability	N	borderline	No IQ test yet Appeared normal	N	Y
Scoliosis	N	N	N	N	N
Ataxia	N	N	N	N	N
Movement disorder	N	N	N	N	Oromotor and limb choreiform movements
Liver disease	N	Y	ND	N	Post mortem: Fatty change, bile ductular proliferation, portal bridging fibrosis
Brain MRI	ND	Equivocally reduced white matter volume	ND	N	Global cerebral and cerebellar atrophy, immature myelination
Muscle imaging	ND	CT: paraspinal and gluteal muscles are mostly affected	CT: mild involvement of gluteal and thigh muscles	CT: atrophy and fatty infiltration of erector spinae, gluteus maximus, adductor longus, and adductor magnus	ND
Transferrin isoforms	Normal	ND	ND	ND	Normal

Other		Liang et al. (5)			Microcephaly Dilated cardiomyopathy
-------	--	---------------------	--	--	---

ND not done Y yes N no CK creatine kinase

Clinical features

Four individuals (individuals 1, 2, 4 and 5) had onset of symptoms (motor difficulties) in the first year of life, (i.e. a congenital onset), while individual 3 had onset after the age of 1 year. All had elevated CK at presentation; individual 2 has been previously described (5), but here we provide immunoanalysis of alpha-dystroglycan glycosylation not previously performed.

All individuals acquired independent ambulation with the exception of individual 5. Cognitive function was impaired in one individual (severely affected infant with CMD, individual 5). The extra muscular features described in previous *TRAPPC11* reports were sought, but were not consistently present. Two individuals had bilateral cataracts (individuals 1 and 2), two had liver involvement (individuals 2 and 5), and one had a choreiform movement disorder with cerebral and cerebellar atrophy on magnetic resonance imaging (MRI) (individual 5; Figure 1). This child additionally had cardiomyopathy. Clinical, imaging and laboratory features for all individuals are summarised in Table 1.

Muscle biopsies revealed dystrophic changes in all five individuals

All 5 individuals underwent a muscle biopsy taken from either the biceps brachialis or the quadriceps (Figure 2). The age at biopsy ranged from 14 months to 4 years. The biopsies revealed dystrophic changes in all five individuals including abnormal size variation, increased internal nuclei, necrosis, regeneration (fetal/developmental myosin positive fibres), fibre splitting, whorling, and fibro-fatty infiltration (individual 1; Figure 2: a-e).

Muscle biopsies revealed abnormalities in dystrophy-associated proteins in all five individuals

Immunoanalysis for a broad panel of dystrophy-associated proteins was performed in all individuals (Figure 2). Individuals 1-4 showed moderate, patchy or mosaic reduction in sarcolemmal labelling with an antibody to alpha-dystroglycan (IIH6, recognising an epitope within the O-glycosylated domain, crucial in binding to laminin alpha-2) (Figure 2: g, p, r, t) and subtle reduction in individual 5 (Figure 2: w). There was variable reduction of several other DAPC proteins including dystrophin and sarcoglycans in two individuals (only individual 1 illustrated; Figure 2 i, j). Unusually, in individual 1, the sarcolemmal depletion of the DAPC proteins was more pronounced in the larger fibres (Figure 2: i-k). These fibres also showed reduced caveolin-3 labelling (Figure 2: n). In all cases, a variable but small number of fibres showed cytoplasmic retention of caveolin-3 and/or dysferlin (Figure 2: o). Labelling for laminin-alpha 2 (300 and 80 kDa forms) and laminin alpha 5 (excluding regenerating fibres) was normal, except for a few larger fibres with an intact basal lamina (normal labelling for laminin gamma 1, a marker of basal lamina integrity, Figure 2: m) showing patchy loss of laminin alpha-2 (Figure 2: l).

Altered alpha-dystroglycan expression and glycosylation in muscle from all five individuals

Quantitative western blotting on muscle lysates using an antibody against alpha-dystroglycan (IIH6) was performed in all cases (Table 2) and showed marked reduction in alpha-dystroglycan expression ($17.8 \pm 8.6\%$ average intensity with an average reduction of 82% in all 5 individuals compared to control). This was accompanied by an aberrant expression pattern comprising 2-3 bands of lower molecular weight, strikingly observed in individual 1 (Figure 3: a). Furthermore, a laminin overlay assay revealed a reduction in the glycosylated form represented by a smear on the blot (Table 2), both in intensity (89% decrease) and in molecular weight in this individual compared to control (Figure 3: b). A similar pattern was observed in the remaining individuals (69% decrease average intensity compared to control).

Table 2: Alpha-dystroglycan western blot and laminin overlay assays in all five individuals

Individual	1	2	3	4	5
αDG WB	12%	14±1.4%	16±4.3%	33±5.6%	14%
LOL	11%	22±12%	21±7%	45%	36%

αDG western blot (αDG WB) and laminin overlay (LOL) assay in the 5 individuals. In both assays the results are expressed as % intensity of the bands (normalised to βDG) compared to control (when the sample had more than 1 band all the values were

added). The % values \pm their standard deviation are shown for the individuals where enough tissue was available to repeat the assays twice.

Flow cytometric analysis

A quantitative flow cytometric assay for alpha-dystroglycan performed on cultured dermal fibroblasts from individual 1 showed no evidence in reduction in the total number of cells expressing IIH6-reactive glycans ($91 \pm 0.5\text{SEM}$ and $98 \pm 0.1\text{SEM}$ for control and individual 1, respectively). Interestingly, we noticed a significant increase (26%) in IIH6 mean fluorescent signal intensity (MFI) compared to a control ($813.8 \pm 35\text{SEM}$ and $1109 \pm 47\text{SEM}$ for control and individual 1, respectively).

Membrane trafficking into and out of the Golgi is delayed in fibroblasts from individual 1

Since TRAPPC11 has been implicated in membrane trafficking in the biosynthetic pathway, we examined fibroblasts from control and the affected individual (individual 1) for the ability to traffic cargo from the endoplasmic reticulum (ER) to and through the Golgi (Figure 4). We first used the RUSH assay (24) to examine the trafficking of two different cargo proteins from the ER to the Golgi. As shown in Figure 4 (a, b), both cargo proteins showed a delay in arrival at the Golgi, consistent with a defect in the early secretory pathway. We also examined the marker VSVG-GFP ts045, a protein that can be conditionally retained in the ER at elevated temperature and released upon downshifting the temperature (25). Similar to the RUSH assay, we noted a delay in the arrival of the fluorescent signal to the Golgi (Figure 4: c). In addition, there was a delay in release of the fluorescent signal from the Golgi, suggesting that import into and export from the Golgi are both affected in the presence of the bi-allelic *TRAPPC11* variant.

Post-mortem findings in individual 5

Individual 5 died at the age of 32 months following cardiovascular complications. A full post-mortem examination was performed. External examination showed right frontal plagiocephaly with a high forehead, downturned mouth, and slightly down-slanting eyes with epicanthic folds. The ears were asymmetric. The skin over the neck was loose, and the nipples were widely spaced. There was peripheral oedema. Internal examination revealed moderate ascites, and large bilateral pleural effusions. There was moderate cardiomegaly (111.7g; expected weight for age 74g) and marked left ventricular dilatation, with fibrosis of the left anterior subepicardial myocardium, extending to the interventricular septum. There were no structural cardiac anomalies. The liver was of normal size and weight but appeared pale and fatty. The muscles appeared pale and flabby, with reduced bulk in the chest and calves. The brain was significantly small for his age (876g; expected weight for age is 1120g). The gyral pattern in the forebrain was normal. The cerebellum was atrophic.

Histology revealed mild myocardial hypertrophy with a distinct wide band of myocyte loss and fibrosis in the left ventricular myocardium with septal extension (Figure 5: a, b). Minor chronic interstitial inflammation, and fatty infiltration in the right ventricle was also noted (data not illustrated). A marked perivenular hepatocyte fatty change and patchy perivenular necrosis associated with bridging portal fibrosis and bile ductular proliferation was seen (Figure 5: l). Dystrophic changes in muscles (psoas, quadriceps, calf pectoralis, and diaphragm) including myopathic size variation, internal nucleation, fibrosis and fatty infiltration were noted (Figure 5: c-k). In the quadriceps there was a dramatic progression of the dystrophic changes from the time of the first biopsy at 14 months, with large areas of complete fibro-fatty replacement adjacent to dystrophic areas in the post-mortem samples (Figure 5: c, d).

Neuropathological examination showed intact cortical organisation in the forebrain, in particular, there was no evidence of neuronal migration defects including cobblestone lissencephaly. There was diffuse neuronal loss, more severe in the outer and middle cortical layers, with neuropil vacuolation. The deep white matter was rarefied, with diffuse cortical and white matter gliosis. The deep grey nuclei were well-formed. There was no evidence of brainstem hypoplasia or dysplasia. The ventricles were dilated. The spinal cord appeared normal.

The cerebellum was hypoplastic, with more severe involvement of the vermis. The histological changes were similar in the vermis and hemispheres. There was diffuse atrophy of the cerebellar folia with widened inter-folia spaces (Figure 6: b, d). Granule cells were virtually absent or very severely depleted (Figure 6: f, g), with depletion of parallel fibres in the molecular layer. The Purkinje cells (PC) were depleted, and most of the surviving neurones showed striking dendritic dystrophy in the form of 'asteroid bodies' which appeared as globular eosinophilic dendritic swellings within the molecular layer (Figure 6: f, g). Immunostaining with a high and low molecular weight neurofilament cocktail antibody (NFC) showed a range of abnormalities, including a chaotic and/or dendritic arbor with misdirected, often swollen proximal primary dendrites, and dystrophic swellings on primary dendrites seen more often distally, showing anomalous dendritic spines radiating in all directions, corresponding to the 'asteroid bodies' (Figure 6: i-m). A proportion of these swellings showed an 'empty core' devoid of any immunoreactivities (Figure 6: m). The dendritic swellings were noted to preferentially accumulate SMI32+ non-phosphorylated neurofilaments (Figure 6: o). The swellings were immunonegative for ubiquitin, p62 and LC3B (markers of autophagy and ubiquitin-proteosomal stress). There were patches of the molecular layer containing a 'disconnected' Purkinje cell arbor devoid of cell bodies within the

depleted Purkinje cell layer underneath the molecular layer (Figure 6: l). There was patchily reduced labelling for alpha-dystroglycan (IIH6) in a proportion of surviving Purkinje cells (Figure 2: z) compared to an age-matched control (Figure 6: x), although, in many other cells, the staining appeared indistinguishable from the control. In contrast, there was virtually no labelling for IIH6-reactive glycans in the dentate nucleus (Figure 6: za) compared to the control (Figure 6: y). TRAPPC11 expression was retained in the residual PCs (Figure 6: zb) and dentate neurones and was comparable to an age-matched control. There was atrophy of the dentate grey ribbon, with neuronal shrinkage (Figure 6: v) and marked activation of CD68+ microglia (Figure 6: w). The cerebellar white matter was rarefied but there was no evidence of axonal dystrophy or dysmyelination, and there was no cerebellar dysplasia.

Discussion

Intracellular transport is mediated by vesicles and multi-protein complexes facilitate this process. Transport protein particle (TRAPP) complex is one such complex and the various component proteins of this complex have a major role in secretory and autophagy pathways including trafficking of various individual and complex proteins (DAPC, sarcoglycan complex, laminin a2, cavins and caveolins) from the ER to the sarcolemma and also from the ER to the Golgi apparatus (11,12).

TRAPPC11, a subunit of the TRAPP complex, is important for complex integrity and anterograde membrane transport from the ER to the ER-Golgi intermediate compartment. Recently a role in autophagy was also suggested (13).

At least 18 individuals with *TRAPPC11* mutations have been reported, ranging from the classical LGMD phenotype at the milder end of the spectrum (14), with the clinical course complicated in some instances by scoliosis, or mild intellectual disability and cataracts (3). At the severe end of the spectrum, individuals with CMD with variable degrees of extra muscular involvement have been described (4, 5), including the description of individuals with achalasia, alacrimia, intellectual disability, and cerebral or cerebellar atrophy on brain MRI (9). A phenotype overlapping congenital disorder of glycosylation (CDG) type II was described in a child with neonatal hypotonia, cholestasis, thrombocytopenia, nephropathy, cerebral atrophy and a combined defect of N- and O-linked glycosylation (15).

Previous studies in mammalian cellular models elucidated the crucial role of TRAPPC11 in maintaining the integrity of the TRAPPIII complex (16). This work also established TRAPPC11 as a bonafide component of human TRAPP, with a role in the early secretory pathway. In extensive functional studies on fibroblasts from individuals carrying *TRAPPC11* mutations, Bogershausen et al (3) demonstrated fragmented Golgi, delayed trafficking out of the Golgi, and abnormally glycosylated LAMP1 and LAMP2 proteins. The zebrafish model of *TRAPPC11*-related disease showed impaired N-linked glycosylation, with compensatory upregulation in several glycosylation-related genes, including the dystroglycanopathy-related genes *GMPPB*, *DPM1*, *DPM2*, and *DPM3* (17). Matalonga et al (15) described the first individual with a multisystem CDG with combined defects in N-linked and O-linked glycosylation and vesicular transport defects in the Golgi due to *TRAPPC11* mutations. There is a further precedent for Golgi dysfunction causing multisystem disease and abnormal glycosylation exemplified by mutations in the genes encoding the COG (conserved oligomeric Golgi) complex, a membrane trafficking complex that localises to the Golgi (18). Dystroglycanopathies include muscular dystrophy and structural involvement of the brain and eye at the severe end of the spectrum. This is due to defective linkage of the sarcolemma to the extracellular matrix (ECM) ligands that occurs via the O-linked mannosylated glycan epitope of alpha-dystroglycan (2). The molecular genetic background is diverse, and defects in genes (*DOLK*, *DPM1*, *DPM2*, *DPM3*, *GMPPB*) involved in dolichol-P-mannose (dol-P-man) synthesis result in N-glycosylation and O-mannosylation defects (hypoglycosylation) of alpha-dystroglycan resulting in dystroglycanopathy (19-21). Recently, Larson et al (23) described one individual with CMD associated with *TRAPPC11* mutations, hypoglycosylation of alpha-dystroglycan and abnormal membrane trafficking to and from the Golgi. This study identified a potential link between TRAPPC11 and the dystroglycanopathies via the role of TRAPPC11 in the trafficking and glycosylation of dystroglycan in the Golgi. More recently, hypoglycosylation of alpha-dystroglycan was described (24) in siblings with *TRAPPC11*-associated LGMD and hepatopathy.

In the present study, all 5 individuals underwent a muscle biopsy providing an opportunity for detailed pathology studies. The biopsies revealed dystrophic changes and consistent but variable reduction of alpha-dystroglycan hypoglycosylation. Interestingly in one individual there was a rapid progression of dystrophic changes between the biopsy taken at 14 months and following post-mortem examination of the same muscle at 32 months. Immunohistochemical analysis revealed patchy mosaic mild-to-moderate reduction in sarcolemmal labelling for IIH6-reactive glycans on alpha-dystroglycan. Quantitative immunoblotting for alpha-dystroglycan showed severe hypoglycosylation in all cases, accompanied by significant reduction of laminin binding in overlay studies, thereby unequivocally demonstrating glycosylation defects. Conversely, quantitative analysis of alpha-dystroglycan from cultured dermal fibroblasts in individual 1 did not demonstrate a reduction, but instead, an increase compared to the control. A similar lack of abnormal labelling in fibroblasts was observed by Larson et al (23) in both their individuals. This may suggest that there are tissue-specific differences in TRAPPC11-mediated Golgi processing and trafficking of alpha-dystroglycan. A similar discrepancy has been reported in other genes implicated in dystroglycanopathies (25, 26). The defective traffic into and out of the Golgi seen in our membrane trafficking assays is consistent with what has been noted for other

TRAPPC11 variants (refs 3, 9, 23). In all our cases, we also documented variable, mildly reduced uneven labelling for dystrophin and/or DAPC proteins. This could be secondary to the reduced labelling for alpha-dystroglycan. In individual 1, there was also patchy reduction in sarcolemmal labelling for caveolin-3, and sarcoplasmic retention of caveolin-3 and dysferlin in a number of non-regenerating, non-necrotic fibres. Caveolin-3 and dysferlin are not part of the DAPC, and sarcolemmal labelling is normally retained in cases with primary or secondary reduction of one or more DAPC proteins. While cytoplasmic retention of caveolin-3 and dysferlin can be observed in regenerating/immature fibres in a variety of dystrophic and/or inflammatory pathologies, the observed cytoplasmic retention in non-regenerating fibres in the biopsy from individual 1 appears consistent with a wider role for the TRAPP complex in membrane trafficking of proteins (DAPC and non-DAPC) to the sarcolemma and out of the ER. While clinical and imaging studies have previously revealed brain involvement in individuals with *TRAPPC11* mutations, there was no information on its neuropathological basis. Brain involvement with cobblestone lissencephaly including brainstem and cerebellar dysplasia and cysts are well documented in individuals with dystroglycanopathies, indicating a major role of dystroglycan in multiple developmental processes including maintenance of the basement membrane integrity, normal radial glia morphology, organisation of neocortical proliferation, and cortical plate lamination (27-29).

Neuropathological examination of the brain in individual 5 with severe CMD revealed notable differences to the structural brain abnormalities associated with the 'classic' dystroglycanopathies. The brain was globally small, but with no evidence of neuronal migration defects in the forebrain. There was marked cerebellar hypoplasia/cerebellar atrophy (CA/CH). An absolute distinction between CA/CH is difficult in absence of serial imaging (30). Histologically, there was no evidence of the neuronal migration defects described in the 'classic' dystroglycanopathies. Instead, we noted a virtually complete loss of the granule cells with accompanying moderate, patchy Purkinje cell loss and a remarkable dendritic dystrophy affecting surviving Purkinje cells. Morphologically, these changes are strikingly similar to the descriptions of primary degeneration of the granular layer of the cerebellum (Norman type) from the pre-molecular era (31). Subsequently, it was suggested that the diseases described by Norman and Jaeken are the same pathological entity, with cerebellar pathology identical to that observed in *PMM2*-related CDG (32). Aronica et al (33) reported post-mortem findings from another case of *PMM2*-related CDG1a, with isolated CA/CH, granule cell depletion, Purkinje cell loss, and morphological changes in the surviving Purkinje cell dendritic arbor. *PMM2*-CDG is a frequent cause of cerebellar ataxia (34) and pathological findings suggest an early-onset atrophic process rather than primary hypoplasia (35). Taken together, these neuropathological findings in our case closely resemble brain involvement in CDG, in particular *PMM2*-CDG, rather than classic dystroglycanopathies. Immunostaining revealed the presence of IIH6-reactive glycans in Purkinje cells, albeit reduced compared to age-matched control, and a virtually total loss of staining in the dentate neurones. Our data provides additional evidence of the overlapping phenotype between dystroglycanopathies and CDG, as previously described in a single case with combined O and N glycosylation defects in a child with neonatal hypotonia, cholestasis, thrombocytopenia, nephropathy, cerebral atrophy [15]. Glycosylation analysis of serum transferrin was normal in this individual (not shown), but analysis of glycoepitopes of secreted proteins may not be sensitive in detection of tissue-specific defects (23).

Conclusions

The present case studies further consolidate recessive *TRAPPC11* mutations as being causally associated with muscular dystrophies of different clinical severity and hypoglycosylation of alpha-dystroglycan. The CNS shows a lack of the classic neuronal migration defects of alpha-dystroglycanopathies, but instead a distinctive type of cerebellar neurodegeneration with remarkable similarities to the cerebellar pathology seen in *PMM2*-CDG. The multisystem involvement with cardiomyopathy and steatohepatitis shows further phenotypic overlap with CDGs. Future work with a focus on animal models to unravel tissue-specific differences in *TRAPPC11*-mediated processing of N- and O-linked glycans should be helpful in discerning the molecular mechanisms of *TRAPPC11*-associated disease.

List Of Abbreviations

TRAPP, ER, CK, PC, CDG, CMDs, LGMDs, DAPC, DDD, MRI, MFI, NFC, ECM, CA/CH, ND, Y, N

Declarations

Ethics approval and consent to participate

Informed consent was obtained from the legal guardians of all individuals described in this study. This study was performed in line with the principles of the Declaration of Helsinki. All human tissues in this study were acquired and processed under appropriate consent and institutional research ethics cover (REC reference: 13/LO/1894 (NRES Committee London). Whole exome sequence was performed on Patient 5 as part of the Deciphering Developmental Disorders (DDD) Study (Cambridge South REC ref: 10/H0305/83 and Republic of Ireland REC ref: GEN/284/12).

Consent for publication

All data depicted in this study including radiology and pathology images has been fully anonymised. Further informed consent for publication was obtained from the legal guardians of the individuals described, and can be made available.

Availability of data and materials

All data generated or analysed during this study are included in this manuscript.

Competing interests

The authors declare that they have no competing interests.

Funding

We acknowledge the financial support from the European Community's Seventh Framework Programme (FP7/2007-2013) funded grant "Integrated European –omics research project for diagnosis and therapy in rare neuromuscular and neurodegenerative diseases (NEUROMICS)" (grant agreement number 2012-305121); the Muscular Dystrophy UK Grant on Gene Identification (Ref: 18GRO-PG24-0271) to Francesco Muntoni, and the NIHR Great Ormond Street Hospital Biomedical Research Centre, UCL GOS Institute of Child Health & Great Ormond Street Hospital Trust, London, UK. Francesco Muntoni is supported by the National Institute for Health Research Biomedical Research Centre at Great Ormond Street Hospital for Children NHS Foundation Trust and UCL. The support of Muscular Dystrophy UK, MRC and BRC Neuromuscular Centre Biobank and NHS England Highly Specialised Services to the Dubowitz Neuromuscular Centre is gratefully acknowledged. The Deciphering Developmental Disorders research study is commissioned by the Health Innovation Challenge Fund (grant number HICF-1009-003), a parallel funding partnership between Wellcome Trust and the Department of Health, and the Wellcome Sanger Institute (grant number WT098051). The research team acknowledges the support of the National Institute for Health Research, through the Comprehensive Clinical Research Network. Michael Sacher is supported by grants from the Canadian Institutes of Health Research (grant number 159645) and the Natural Sciences and Engineering Research Council of Canada (grant number RGPIN/04385). The views expressed are those of the author(s) and not necessarily those of the institutions or funding bodies.

Authors' contributions

Francesco Muntoni, Michael Sacher, Ichizo Nishino, Pinki Munot and Rahul Phadke contributed to the study conception and design. Material preparation, data collection and analysis were performed by Pinki Munot, Nadine McCrea, Silvia Torelli, Adnan Manzur, Caroline Sewry, Pierpaolo Ala, Irina Zaharieva, Nicola Ragge, Helen Roper, Tamas Marton, Phil Cox, Miroslav Milev, Michael Sacher, Wen-Chen Liang, Shinsuke Maruyama, Ichizo Nishino, Rahul Phadke and Francesco Muntoni. Darren Chambers and Lucy Feng provided technical assistance. The first draft of the manuscript was written by Pinki Munot, Nadine McCrea and Rahul Phadke, and all authors commented on previous versions of the manuscript. All authors read and approved the final manuscript.

Acknowledgements

We are grateful to the families of the individuals described in this study for extending their support. We acknowledge the financial support from: the European Community's Seventh Framework Programme (FP7/2007-2013) funded grant "Integrated European –omics research project for diagnosis and therapy in rare neuromuscular and neurodegenerative diseases (NEUROMICS)"; Muscular Dystrophy UK; NIHR Great Ormond Street Hospital Biomedical Research Centre, UCL GOS Institute of Child Health & Great Ormond Street Hospital Trust, London, UK; MRC and BRC Neuromuscular Centre Biobank UK; NHS England Highly Specialised Services; Deciphering Developmental Disorders research study commissioned by the Health Innovation Challenge Fund, a parallel funding partnership between Wellcome Trust and the Department of Health, and the Wellcome Sanger Institute UK; National Institute for Health Research, through the Comprehensive Clinical Research Network, UK; Canadian Institutes of Health Research and the Natural Sciences and Engineering Research Council of Canada. The views expressed are those of the author(s) and not necessarily those of the institutions or funding bodies.

References

1. Laval SH, Bushby KMD. Limb-girdle muscular dystrophies—from genetics to molecular pathology. *Neuropathology and applied neurobiology*. 2004;30(2):91-105.
2. Mercuri E, Bonnemann CG, Muntoni F. Muscular dystrophies. *Lancet (London, England)*. 2019;394(10213):2025-38.
3. Bogershausen N, Shahrzad N, Chong JX, von Kleist-Retzow J-C, Stanga D, Li Y, et al. Recessive TRAPPC11 mutations cause a disease spectrum of limb girdle muscular dystrophy and myopathy with movement disorder and intellectual disability. *American journal of human genetics*. 2013;93(1):181-90.

4. Milev MP, Stanga D, Schanzer A, Nascimento A, Saint-Dic D, Ortez C, et al. Characterization of three TRAPPC11 variants suggests a critical role for the extreme carboxy terminus of the protein. *Scientific reports*. 2019;9(1):14036.
5. Liang W-C, Zhu W, Mitsuhashi S, Noguchi S, Sacher M, Ogawa M, et al. Congenital muscular dystrophy with fatty liver and infantile-onset cataract caused by TRAPPC11 mutations: broadening of the phenotype. *Skelet Muscle*. 2015;5:29.
6. Dubowitz VOASCA. *MUSCLE BIOPSY : a practical approach*. [S.l.]: ELSEVIER HEALTH SCIENCES; 2019.
7. Brockington M, Torelli S, Sharp PS, Liu K, Cirak S, Brown SC, et al. Transgenic overexpression of LARGE induces alpha-dystroglycan hyperglycosylation in skeletal and cardiac muscle. *PLoS one*. 2010;5(12):e14434.
8. Stevens E, Torelli S, Feng L, Phadke R, Walter MC, Schneiderat P, et al. Flow cytometry for the analysis of α -dystroglycan glycosylation in fibroblasts from patients with dystroglycanopathies. *PLoS One*. 2013;8(7):e68958.
9. Koehler K, Milev MP, Prematilake K, Reschke F, Kutzner S, Juhlen R, et al. A novel TRAPPC11 mutation in two Turkish families associated with cerebral atrophy, global retardation, scoliosis, achalasia and alacrima. *J Med Genet*. 2017;54(3):176-85.
10. Milev MP, Grout ME, Saint-Dic D, Cheng Y-HH, Glass IA, Hale CJ, et al. Mutations in TRAPPC12 Manifest in Progressive Childhood Encephalopathy and Golgi Dysfunction. *American journal of human genetics*. 2017;101(2):291-9.
11. Busija AR, Patel HH, Insel PA. Caveolins and cavins in the trafficking, maturation, and degradation of caveolae: implications for cell physiology. *Am J Physiol Cell Physiol*. 2017 Apr 1;312(4):C459-C477.
12. Sandonà D, Betto R. Sarcoglycanopathies: molecular pathogenesis and therapeutic prospects. *Expert Rev Mol Med*. 2009 Sep 28;11:e28.
13. Stanga D, Zhao Q, Milev MP, Saint-Dic D, Jimenez-Mallebrera C, Sacher M. TRAPPC11 functions in autophagy by recruiting ATG2B-WIPI4/WDR45 to preautophagosomal membranes. *Traffic (Copenhagen, Denmark)*. 2019;20(5):325-45.
14. Wang X, Wu Y, Cui Y, Wang N, Folkersen L, Wang Y. Novel TRAPPC11 Mutations in a Chinese Pedigree of Limb Girdle Muscular Dystrophy. *Case Rep Genet*. 2018;2018:8090797.
15. Matalonga L, Bravo M, Serra-Peinado C, Garcia-Pelegri E, Ugarteburu O, Vidal S, et al. Mutations in TRAPPC11 are associated with a congenital disorder of glycosylation. *Human mutation*. 2017;38(2):148-51.
16. Scrivens PJ, Noueihed B, Shahrzad N, Hul S, Brunet S, Sacher M. C4orf41 and TTC-15 are mammalian TRAPP components with a role at an early stage in ER-to-Golgi trafficking. *Mol Biol Cell*. 2011;22(12):2083-93.
17. DeRossi C, Vacaru A, Rafiq R, Cinaroglu A, Imrie D, Nayar S, et al. trappc11 is required for protein glycosylation in zebrafish and humans. *Mol Biol Cell*. 2016;27(8):1220-34.
18. Freeze HH, Eklund EA, Ng BG, Patterson MC. Neurology of inherited glycosylation disorders. *The Lancet Neurology*. 2012;11(5):453-66.
19. Lefeber DJ, de Brouwer APM, Morava E, Riemersma M, Schuurs-Hoeijmakers JHM, Absmanner B, et al. Autosomal recessive dilated cardiomyopathy due to DOLK mutations results from abnormal dystroglycan O-mannosylation. *PLoS genetics*. 2011;7(12):e1002427.
20. Yang AC, Ng BG, Moore SA, Rush J, Waechter CJ, Raymond KM, et al. Congenital disorder of glycosylation due to DPM1 mutations presenting with dystroglycanopathy-type congenital muscular dystrophy. *Molecular genetics and metabolism*. 2013;110(3):345-51.
21. Lefeber DJ, Schonberger J, Morava E, Guillard M, Huyben KM, Verrijp K, et al. Deficiency of Dol-P-Man synthase subunit DPM3 bridges the congenital disorders of glycosylation with the dystroglycanopathies. *American journal of human genetics*. 2009;85(1):76-86.
22. Raphael AR, Couthouis J, Sakamuri S, Siskind C, Vogel H, Day JW, et al. Congenital muscular dystrophy and generalized epilepsy caused by GMPPB mutations. *Brain research*. 2014;1575:66-71.
23. Larson AA, Baker PR, 2nd, Milev MP, Press CA, Sokol RJ, Cox MO, et al. TRAPPC11 and GOSR2 mutations associate with hypoglycosylation of alpha-dystroglycan and muscular dystrophy. *Skelet Muscle*. 2018;8(1):17.
24. Fee DB, Harmelink M, Monrad P, Pyzik E. Siblings With Mutations in TRAPPC11 Presenting With Limb-Girdle Muscular Dystrophy 2S. *Journal of clinical neuromuscular disease*. 2017;19(1):27-30.
25. Jensen BS, Willer T, Saade DN, Cox MO, Mozaffar T, Scavina M, et al. GMPPB-Associated Dystroglycanopathy: Emerging Common Variants with Phenotype Correlation. *Human mutation*. 2015;36(12):1159-63.
26. Carss KJ, Stevens E, Foley AR, Cirak S, Riemersma M, Torelli S, et al. Mutations in GDP-mannose pyrophosphorylase B cause congenital and limb-girdle muscular dystrophies associated with hypoglycosylation of alpha-dystroglycan. *American journal of human genetics*. 2013;93(1):29-41.
27. Bonnemann CG, Wang CH, Quijano-Roy S, Deconinck N, Bertini E, Ferreira A, et al. Diagnostic approach to the congenital muscular dystrophies. *Neuromuscular disorders : NMD*. 2014;24(4):289-311.
28. Myshra TD, Moore SA, Ostendorf AP, Satz JS, Kowalczyk T, Nguyen H, et al. Dystroglycan on radial glia end feet is required for pial basement membrane integrity and columnar organization of the developing cerebral cortex. *Journal of neuropathology and experimental neurology*. 2012;71(12):1047-63.

29. Devisme L, Bouchet C, Gonzales M, Alanio E, Bazin A, Bessieres B, et al. Cobblestone lissencephaly: neuropathological subtypes and correlations with genes of dystroglycanopathies. *Brain : a journal of neurology.* 2012;135(Pt 2):469-82.
30. Poretti A, Boltshauser E. Terminology in morphological anomalies of the cerebellum does matter. *Cerebellum Ataxias.* 2015;2:8.
31. Ferrer I, Sirvent J, Manresa JM, Galofre E, Fernandez-Alvarez E, Pineda M. Primary degeneration of the granular layer of the cerebellum (Norman type). A Golgi study. *Acta neuropathologica.* 1987;75(2):203-8.
32. Pascual-Castroviejo I, Pascual-Pascual SI, Quijano-Roy S, Gutierrez-Molina M, Morales MC, Velazquez-Fragua R, et al. [Cerebellar ataxia of Norman-Jaeken. Presentation of seven Spanish patients]. *Rev Neurol.* 2006;42(12):723-8.
33. Aronica E, van Kempen AAMW, van der Heide M, Poll-The BT, van Slooten HJ, Troost D, et al. Congenital disorder of glycosylation type Ia: a clinicopathological report of a newborn infant with cerebellar pathology. *Acta neuropathologica.* 2005;109(4):433-42.
34. Boddaert N, Desguerre I, Bahi-Buisson N, Romano S, Valayannopoulos V, Saillour Y, et al. Posterior fossa imaging in 158 children with ataxia. *J Neuroradiol.* 2010;37(4):220-30.
35. Antoun H, Villeneuve N, Gelot A, Panisset S, Adamsbaum C. Cerebellar atrophy: an important feature of carbohydrate deficient glycoprotein syndrome type 1. *Pediatric radiology.* 1999;29(3):194-8.

Figures

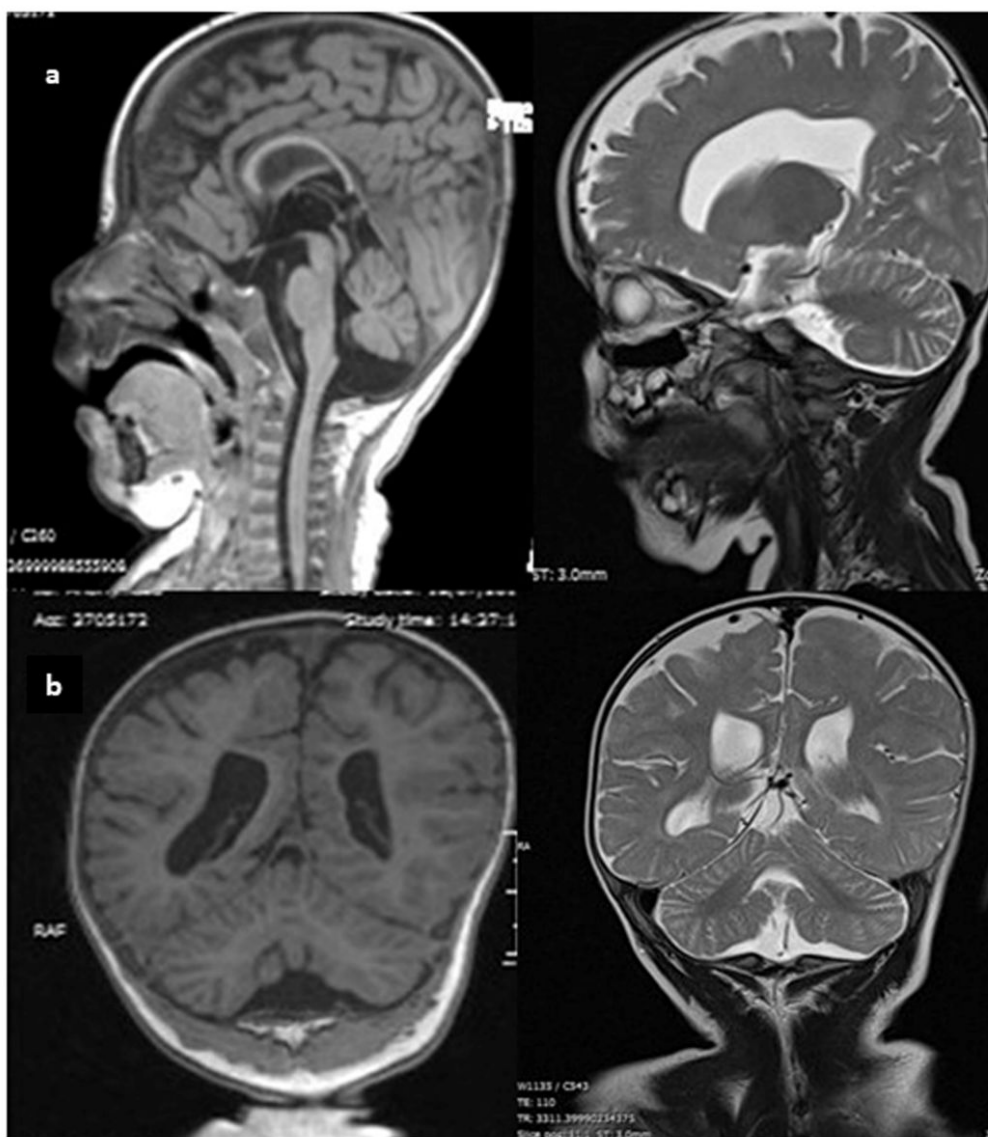


Figure 1

Brain MRI findings in Case 5 MRI of the brain in sagittal (a) and coronal (b) sections demonstrates cerebral and cerebellar atrophy.

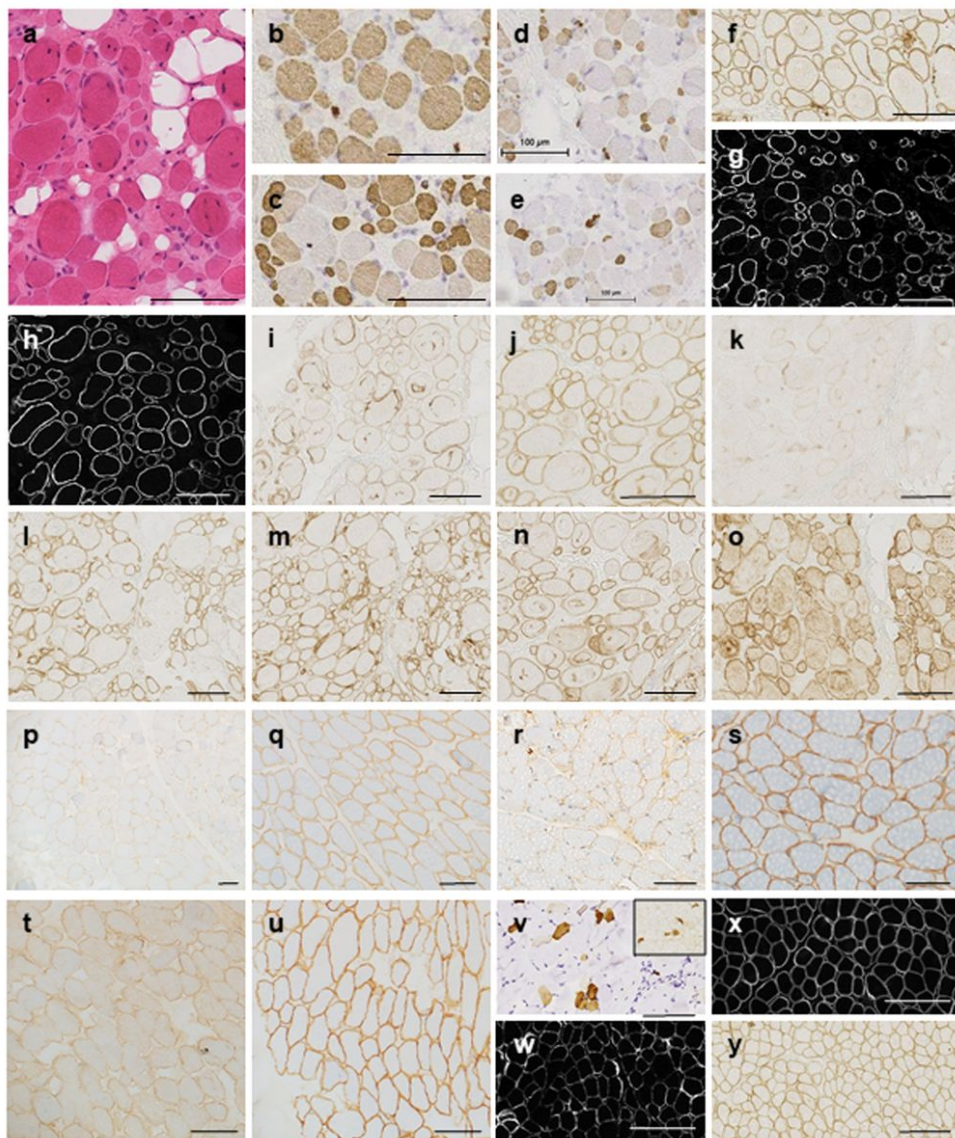


Figure 2

Dystrophic muscle pathology from quadriceps and biceps brachialis biopsies Diagnostic muscle biopsies were performed in all 5 individuals, from the quadriceps (individual 1: a-o and 5: v-y), or the biceps brachialis (individual 2: p, q, 3: r, s and 4: t, u). The biopsy from individual 1 taken at 2 years showed moderate-to-marked dystrophic changes (a). There was overall slow fibre predominance (b). Fast myosin showed considerable co-expression (c) with preferential expression in smaller fibres clustering around larger preferentially slow myosin expressing fibres. There were many fibres of all sizes and intensities expressing fetal (d) and developmental (e) myosins, consistent with a dystrophic pattern. Most fibres retained robust spectrin labelling indicating an intact sarcolemma (f). There was moderate mosaic/uneven depletion of sarcolemmal alpha-dystroglycan (g), with normal expression of beta-dystroglycan (h). C-terminal dystrophin (i) and alpha-sarcoglycan (j) were patchily reduced, and NNOS (k) was markedly depleted. Laminin alpha 2 (300 kDa) was reduced in a few larger fibres (l) that retained laminin gamma a1 labelling (m) suggesting that the basal lamina was intact in these fibres. There was mild uneven labelling for caveolin-3 (n) and several fibres of varying size showed sarcoplasmic retention of dysferlin (o). Sarcolemmal alpha-dystroglycan labelling was moderate-to-severely reduced in individuals 2-4 (p, r, t). Alpha-sarcoglycan was mildly reduced in individual 2 (q), and appeared normal in individuals 3 and 4 (s and u). In individual 5, the dystrophic changes in the biopsy taken at 14 months were subtle, only recognisable due to a dystrophic labelling pattern for fetal (v) and developmental (v, inset) myosins. Reduction of sarcolemmal alpha-dystroglycan labelling in this individual was subtle (w); labelling for dystrophin and other related proteins including beta-dystroglycan (x), alpha-sarcoglycan (y) appeared normal. Scale bar: 1a-1o, 5a-5d = 100 μ m; 2a-4b = 50 μ m

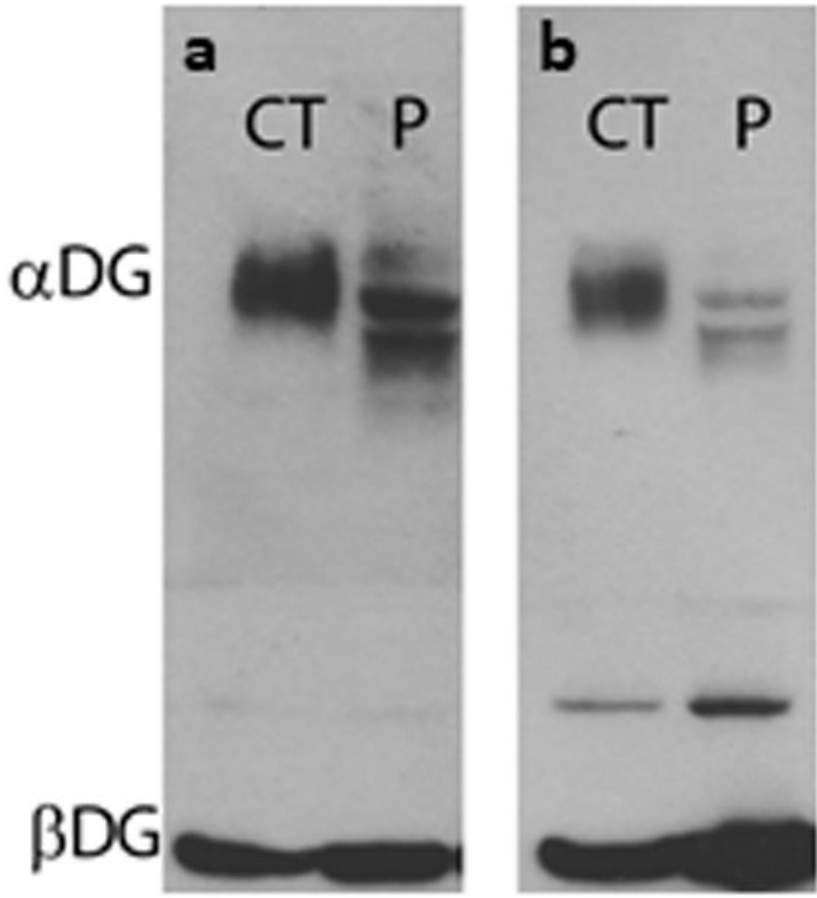


Figure 3

Western blot demonstrates reduced alpha-dystroglycan glycosylation and laminin binding in muscle. Representative image for western blot (a) and laminin overlay assay (b) (individual 1). A reduction in the glycosylated smear of the individual, both in intensity and in molecular weight, was observed compared to the control with antibody IIH6. Three bands are visible in the individual lysate (a) and two of them are also seen with the laminin overlay (b). β-DG was used as a loading protein. α-DG: alpha-dystroglycan, β-DG: beta-dystroglycan, CT: control, P: individual 1

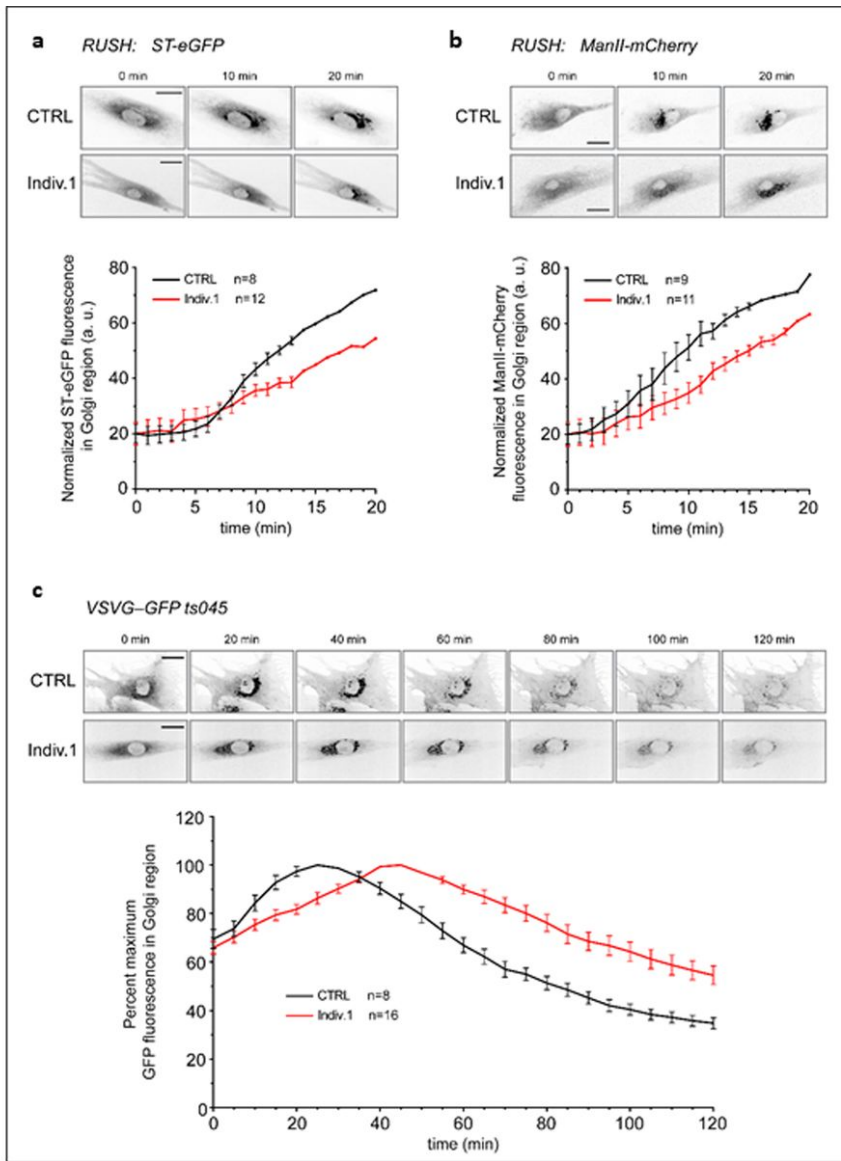


Figure 4

Membrane trafficking is delayed in individual 1 Cells from the TRAPPC11 bi-allelic variant display a defect in membrane trafficking. The RUSH assay was performed in fibroblasts from a control and the affected individual (Individual 1) using sialyl transferase (ST)-eGFP (a) and mannosidase II (ManII)-mCherry (b). The signal in the Golgi was quantified as described previously (Milev et al, 2017) and is plotted beneath the representative images. (c) An assay for the trafficking of VSVG-GFP ts045 into and out of the Golgi of the fibroblasts was performed and quantified as previously described (Koehler et al, 2017). Error bars represent SEM. Bars in the representative images are 20 μm .

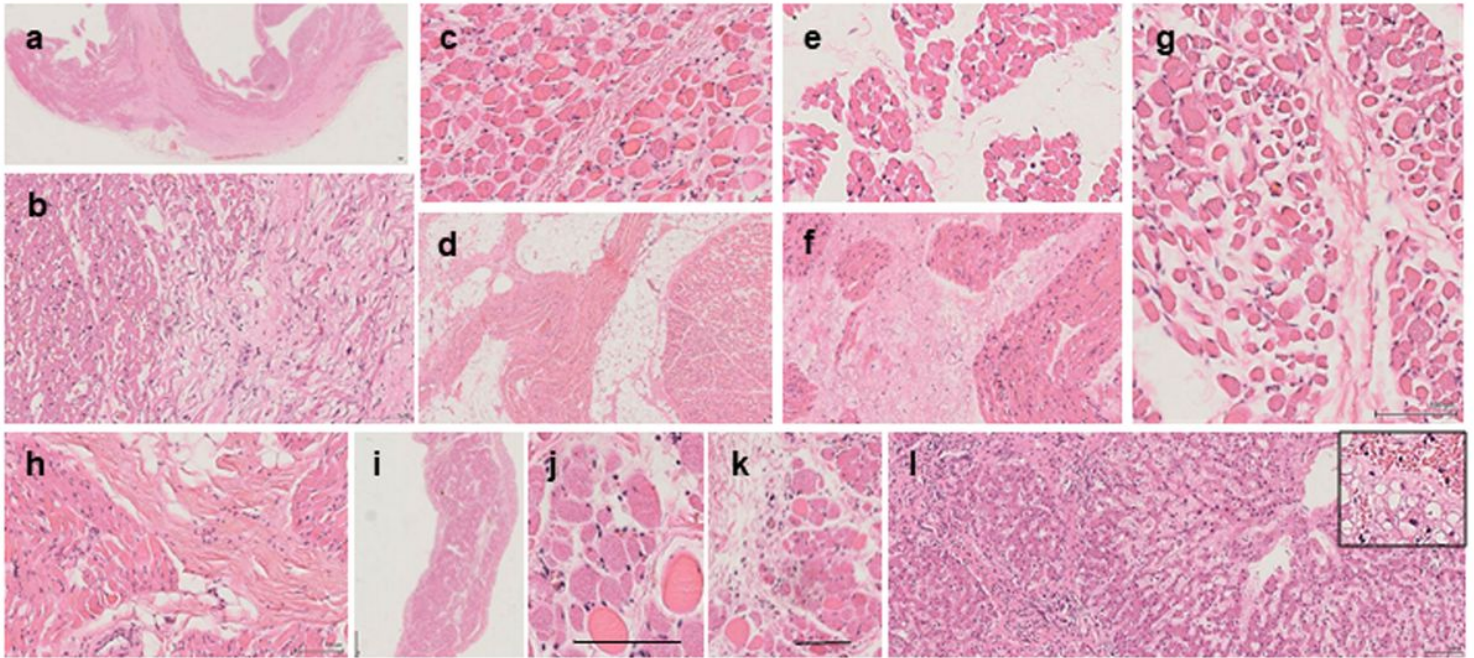


Figure 5

Post mortem systemic pathology in individual 5 Post mortem pathology in individual 5. Heart (a, b), skeletal muscles (c-k) and liver (l). Heamatoxylin and eosin stained section from the left and right ventricle with adjoining septum showed a concentric thick band of fibrosis in the outer and mid-myocardium (a). Higher magnification shows an area of scarring adjacent to mildly hypertrophied cardiomyocytes (b). Marked dystrophic changes were seen in multiple skeletal muscles samples including the quadriceps (c, d), calf (e, f), psoas (g), pectoralis (h) and diaphragm (i-k). There were confluent areas of total fibrofatty replacement in the quadriceps (d) and calf (f). The liver showed marked perivenous changes including sinusoidal congestion and fatty degeneration of hepatocytes with accompanying portal bridging fibrosis and bile ductular proliferation (l). Scale bar: 1, 9, 12 = 1mm; 2-8, 10, 11 = 100 μ m

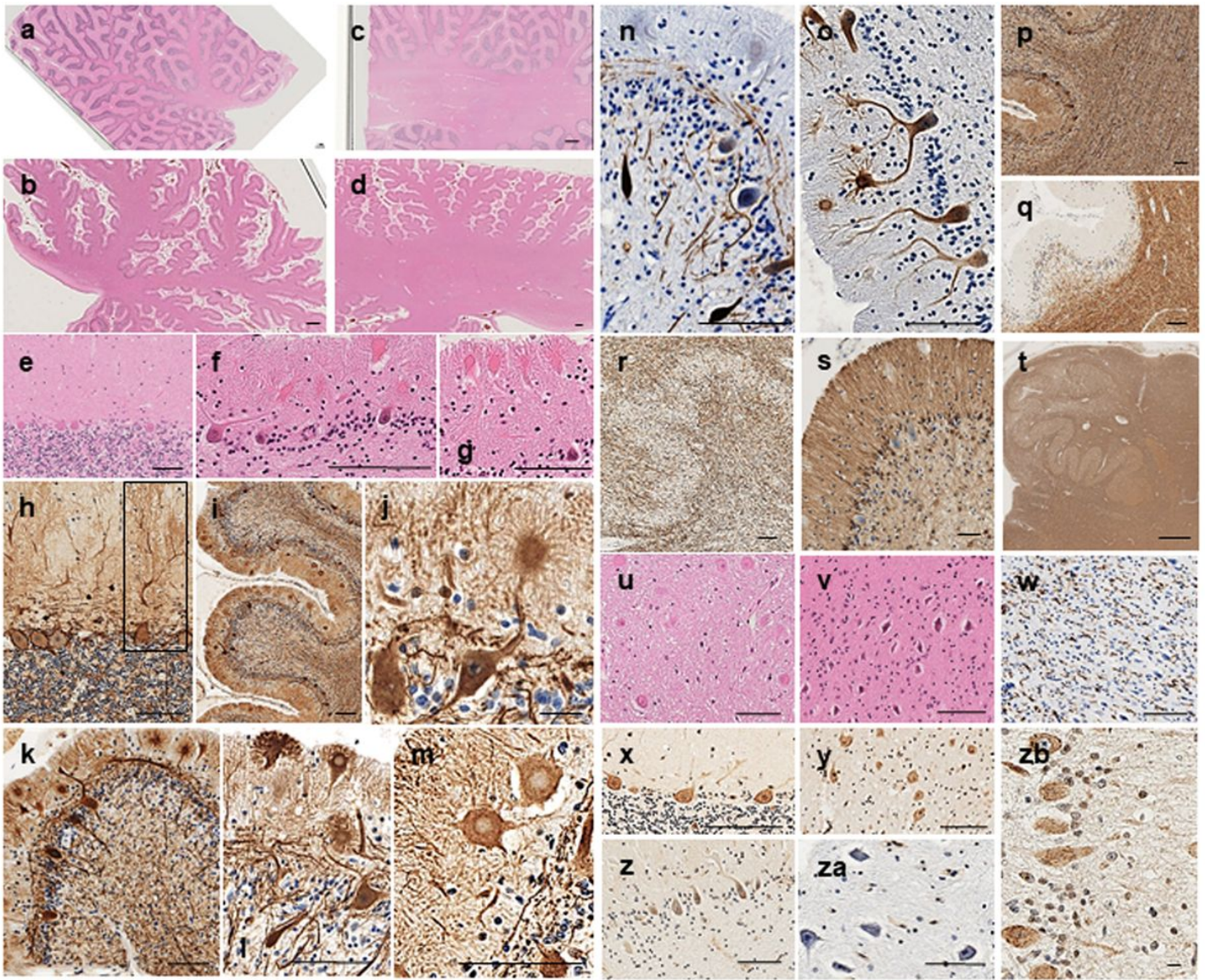


Figure 6

Post mortem pathological findings from the brain in individual 5 Compared to sections from the vermis (a) and hemisphere (c) from an age-matched control, the individual showed marked vermian (b) and hemispheric (d) atrophy of the folia and widened inter-folial spaces. Compared to the control (e) there was sub-total loss of granule cells and frequent, patchy loss of Purkinje cells. Surviving Purkinje cells showed remarkable dendritic dystrophy, with eosinophilic swellings emanating from proximal or distal dendrites within the molecular layer (f, g). Neurofilament cocktail (NFC) staining showed an orderly Purkinje cell dendritic arbor in the control (box, h) with robust network of parallel fibres. In the individual, the surviving Purkinje cells showed abnormally oriented dendrites with thickened primary branches and frequent NFC+ swellings on terminal, and less frequently, proximal primary dendrites with anomalous spines radiating in all directions, so called asteroid bodies. The dendritic arbor was reduced, and there were patches of the molecular layer with 'disconnected' dendritic arbor with absent Purkinje cell bodies (i-m). A proportion of these swellings displayed immunonegative 'empty cores' (m). Staining with antibodies to phosphorylated (SMI31) (n) and non-phosphorylated (SMI32) (o) neurofilaments showed preferential aggregation of non-phosphorylated neurofilaments within the dendritic swellings. There were scattered Purkinje cell axonal swellings or 'torpedoes' aggregating SMI31+ phosphorylated neurofilaments (n). There was commensurate depletion of NFC+ axons and rarefaction of SMI94+ myelinated fibres in the subcortical white matter (p, q) and in the hilum of the dentate nucleus (r). There was prominent GFAP+ Bergmann/radial gliosis within the molecular layer (s). The inferior olivary ribbon in the medulla appeared normal (t). Compared to the control (u), there was marked shrinkage of neurones within the dentate ribbon (v), with brisk CD68+ microglial activation (w). IiH6 alpha-dystroglycan antibody strongly labeled Purkinje cells (x) and dentate neurones (y) in the control. In comparison, IiH6 labeling of Purkinje cells appeared reduced (z), with virtually no labeling of dentate neurones (za) in the individual. There was discernible TRAPPC11 expression in most Purkinje cells in the individual (zb). Scale bar: 1-4, 20 = 1mm; 5-19, 21-28 = 100 µm

Supplementary Files

This is a list of supplementary files associated with this preprint. Click to download.

- [WBsupplementaryfigurelegend.pdf](#)
- [IHCcontrolssupplementaryfigurelegend.pdf](#)